

Precursors and e^\pm pair loading from erupting fireballs

Enrico Ramirez-Ruiz^{1,2}, Andrew I. MacFadyen² and Davide Lazzati¹

1. *Institute of Astronomy, Madingley Road, Cambridge, CB3 0HA, UK.*

2. *Department of Astronomy and Astrophysics, University of California, Santa Cruz, CA 95064, USA.*

ABSTRACT

Recent observations suggest that long-duration γ -ray bursts and their afterglows are produced by highly relativistic jets emitted in core-collapse explosions. As the jet makes its way out of the stellar mantle, a bow shock runs ahead and a strong thermal precursor is produced as the shock breaks out. Such erupting fireballs produce a very bright γ -ray precursor as they interact with the thermal break-out emission. The prompt γ -ray emission propagates ahead of the fireball before it becomes optically thin, leading to e^\pm pair loading and radiative acceleration of the external medium. The detection of such precursors would offer the possibility of diagnosing not only the radius of the stellar progenitor and the initial Lorentz factor of the collimated fireball, but also the density of the external environment.

Key words: gamma-rays: bursts – stars: supernovae – X-rays: sources

1 INTRODUCTION

A generic scheme for a cosmological γ -ray burst (GRB) model has emerged in the last few years (see Mészáros 2001 for a review). According to this scheme the observed γ -rays are emitted when a relativistic energy flow is converted to radiation (Rees & Mészáros 1992; 1994; Paczyński & Xu 1994; Katz 1994; Sari & Piran 1995). Possible forms of the energy flow are kinetic energy of relativistic particles or electromagnetic Poynting flux (Rees 1999). This energy must be converted to radiation in an optically thin region, as the observed bursts are not thermal. The ultimate energy source of this relativistic outflow is the gravitational energy release associated with temporary mass accretion onto a black hole, which results either from the collapse of a massive rotating star (Woosley 1993; Paczyński 1998; MacFadyen & Woosley

1999; MacFadyen, Woosley & Heger 2001) or from a compact merger (Lattimer & Schramm 1976; Eichler et al. 1989; Ruffert et al. 1997; Klužniak & Lee 1998; Lee & Klužniak 1999).

For the long burst afterglows localized so far, the host galaxies show signs of ongoing star formation activity necessary for the presence of young, massive progenitor stars (Fruchter et al. 1999). The physical properties of the afterglows (Kulkarni et al. 1998; Fruchter 1999; Ramirez-Ruiz, Trentham & Blain 2002), their locations at a few kpc from the centre of the host galaxies (Bloom, Kulkarni & Djorgovski 2001), the presence of iron line features (GRB 991216, Piro et al. 2000; GRB990705, Amati et al. 2000), and the evidence of a supernova component detected several weeks after the burst (GRB980326, Bloom et al. 1999; GRB970228, Reichart 1999; GRB 000911, Lazzati et al. 2001), all give strong support to the idea that the most common GRBs are linked to the cataclysmic collapse of massive stars into black holes. In this case, the γ -rays are thought to be produced in shocks occurring after the relativistic jet has broken free from the stellar envelope, whose density is reduced along the rotation axis due to an early phase of accretion (MacFadyen & Woosley 1999 and MacFadyen, Woosley & Heger 2001; hereinafter MW99 and MWH01 respectively). A strong terminal wave breaking out of the envelope is expected to produce a transient thermal emission that should appear as a precursor signal prior to the observed GRB (Colgate 1974; Chevalier 1982; MWH01; Mészáros & Waxman 2001).

In this paper we explore the interaction of such erupting fireballs with the shock breakout emission. We show that a substantial fraction of the fireball energy can be converted into a collimated, bright γ -ray precursor via the Compton drag process (Lazzati et al. 2000 and Ghisellini et al. 2001; hereinafter L00 and G01 respectively). The prompt γ -rays would propagate ahead of the fireball before it becomes optically thin, leading to e^\pm pair production and thus an associated deposition of momentum into the external medium (Madau & Thompson 2000 and Thompson & Madau 2000; hereinafter MT00 and TM00 respectively). In this scenario, the effects of e^\pm pair production can be substantial, increasing the radiative efficiency of the blast wave and modifying the early dynamics of the fireball (in contrast with Dermer & Böttcher 2000; Madau, Blandford & Rees 2000; Mészáros, Ramirez-Ruiz & Rees 2001 and Belobodorov 2002; all of whom consider the effects of such mechanisms beyond the radius at which the relativistic fireball becomes optically thin to scattering). We suggest that detailed observation of this prompt emission provides a potential tool for diagnosing the radius of the stellar progenitor and the initial Lorentz factor of the fireball. It also provides a means for probing the external environment surrounding the stellar progenitor and the ra-

dial distance at which the observed γ -rays are produced. We assume $H_0 = 65 \text{ kms}^{-1}\text{Mpc}^{-1}$, $\Omega_m = 0.3$, $\Omega_\Lambda = 0.7$.

2 ERUPTING FIREBALLS

Numerical simulations of rotating helium stars in which iron core collapse does not produce a successful traditional neutrino-powered explosion (MW99; Aloy et al. 2000; MWH01) have identified a range of stellar progenitors and initial conditions in which a jet would not be able to break free from its stellar cocoon. This is expected in a large fraction of cases where the stellar envelope is too thick, for example in stars with small radiative mass-loss. A highly relativistic jet is likely to escape if the star loses its hydrogen envelope before collapsing and if the jet produced by the accretion maintains its energy for longer than it takes the jet to reach the surface of the star (MW99). Otherwise, acceleration of the explosion debris to a sufficiently high Lorentz factor ($> 10^2$, Mészáros & Rees 1997) is unlikely and an asymmetric supernovae like SN 1998bw may result (MWH01).

A collimated fireball propagating inside a funnel cavity would be stopped by the envelope when its momentum flux is insufficient to accelerate the impacted stellar mantle to a speed comparable to its own. The jet would then be stalled at a distance $\approx \sqrt{L_j/(\Omega \rho_{\text{env}} v_j^3)}$ (Wheeler et al. 2000), where L_j is the total luminosity of the jet, Ω its collimation solid angle and ρ_{env} the density along the rotation axis of the star. At this distance, the relativistic jet is abruptly decelerated to $\Gamma \approx 1$. In order to break through the star, the energy injected into the envelope, $E_j = L_j \Delta t_j$, should be enough to unbind the impacted envelope material. Thus, inside a rotating massive star whose core has collapsed (leading to a central black hole), gas fall-back would drive for a time $\Delta t_j = r_*/\bar{v}_h \approx 10^3 r_{*,13} \text{ s}$ a slowly advancing standoff shock inside the envelope¹ (MW99; MWH01; see Fig. 1a), where the average speed of the jet head \bar{v}_h is about $c/2$ (Aloy et al. 2000; Zhang et al., 2001, in preparation). For small opening angles $\theta \ll 1$, the thickness of the shocked plasma shell is² $\Delta \approx \sqrt{3} \theta r_*/8$, where r_* is the stellar radius (Mészáros & Waxman 2001). The bow shock of the jet will heat the shocked plasma, converting a large fraction of its internal energy into radiation

¹ The shocked jet plasma and the shocked stellar plasma propagate at a subrelativistic velocity $\Gamma_h \approx 1 \ll \Gamma_j$ up to the H envelope radius. During the propagation in the H envelope, the density drops and the jet can accelerate to relativistic speed (MWH01, Mészáros & Waxman 2001). Here we adopt the convention $Q = 10^x Q_x$, using cgs units.

² Calculated by balancing the particle flux across the standoff shock with the tangential flux of particles leaving the cylinder of height Δ .

(Fig. 1b). The high opacity of the plasma shell would cause the radiation to thermalize with a black body emission at a temperature³ (Mészáros & Waxman 2001)

$$T_p \approx 0.3 \left[\frac{E_{j,51}}{r_{*,13}^2 \Delta t_{j,2} \theta_{-1}^2} \right]^{1/4} \text{keV.} \quad (1)$$

This emission would not be appreciably beamed. Once the strong shock wave breaks the stellar surface, the temperature of the shocked plasma decreases roughly as a power-law $T(t) \approx T_p(1 + 3ct/\Delta)^{-1/3}$. These analytical estimates are consistent with numerical results (MWH01).

A relativistic collimated fireball may result if the engine operates for a sufficiently long time to allow the standoff shock (i.e. the jet head) to break out of the surface of the star. High Lorentz factors ($\Gamma > 100$) can be achieved if the jet continues to be powered after jet break out. The column of stellar material pushed ahead of the jet ($0.1 - 1 M_\odot$) escapes the star and expands sideways, leaving a decreasing amount of material ahead of the jet. This allows the hot, low-density jet plasma with moderately relativistic bulk velocity to accelerate to Lorentz factors determined by the energy loading per baryon in the jet (see Zhang et al. 2001, in preparation). The jet remains physically beamed due to relativistic effects. The shocked plasma temperature at the time at which the fireball crosses the surface ($t \approx \Delta/c$) is $T_s \approx T_p/4^{1/3}$. Thus, the erupting fireball escapes the stellar envelope while interacting with very dense soft photon emission with typical energy $\Theta_s = kT_s/(m_e c^2)$ (Fig. 1c). A fraction $\approx \min(1, \tau_j)$ of the photons are scattered by the inverse Compton effect to energies $\approx 2\Gamma_0^2 \Theta_s$, where τ_j is the Thomson optical depth of the collimated fireball and we assume that a constant Γ_0 has been reached at the stellar surface. The radius of transparency of the fireball is

$$r_\tau \approx 2 \times 10^{14} \theta_{-1}^{-1} \Gamma_{0,2}^{-1/2} E_{j,51}^{1/2} \text{ cm.} \quad (2)$$

Due to relativistic aberration, the scattered photons propagate in a narrow $1/\Gamma$ beam. The net amount of energy E_{ic} extracted by the Compton drag process is $\approx \Gamma^2 \min(1, \tau_j) \Delta \pi(\theta r)^2 a T_s^4$,

³ This estimate assumes that the fireball propagates in a funnel along the rotation axis of the star, which is supported by rotation in the transverse direction and thus jet sideways expansion inside the stellar envelope does not occur. Alternatively, if sideways expansion of the jet material takes place before leaving the stellar surface, most of the energy output could be deposited into a cocoon of relativistic plasma surrounding the jet (Ramirez-Ruiz, Celotti & Rees 2001, in preparation). In this case, the shocked plasma internal energy converted to radiation is smaller and thus the black body radiation temperature may be lower.

where $\Delta\pi(\theta r)^2$ is the volume filled by the soft photon radiation. The Compton drag process can be very efficient in extracting energy from the collimated fireball

$$\xi = \frac{E_{\text{ic}}}{E_j} \approx \theta_{-1} r_{*,13} \Delta t_{j,2}^{-1} \Gamma_{0,2}^2 \quad r < r_\tau \quad (3)$$

even for jets erupting from stars with small radii $r_* < 10^{12}$ cm. Note that the Compton drag process limits the maximum speed of expansion so that $\xi < 1$ (L00). When the fireball becomes transparent, the amount of scattered photons is correspondingly reduced, and the process becomes less efficient. Each seed photon is boosted by $\approx \Gamma^2$ in frequency, yielding a spectrum peaking at

$$h\nu \approx 2\Gamma_0^2(3kT_s) \approx 11\Gamma_{0,2}^2 \frac{E_{j,51}^{1/4}}{r_{*,13}^{1/2} \Delta t_{j,2}^{1/4} \theta_{-1}^{1/2}} (1+z)^{-1} \text{MeV.} \quad (4)$$

The observed variability time scale is related to the typical size Δ of the shocked plasma region containing the thermal photon field, its curvature r_* , and the mean free path λ of a photon inside the fireball. The observed time-scale is hence given by $\max(\frac{\lambda}{c}, \frac{r_*}{c\Gamma_0^2}, \frac{\Delta}{c\Gamma_0^2})$, where $\lambda \sim 10^{10} (r_{*,13}\theta_{-1})^2 \Gamma_{0,2} t_{j,2} E_{j,51}^{-1}$ cm. For large Lorentz factors, the duration is dominated by the mean free path term, while for slow fireballs the curvature is more important. Taking into account the conservation of the number of photons and the increase by a factor $2\Gamma_0^2$ of the photon energy, the peak luminosity of the boosted component is

$$L_{\text{ic}} \approx 2^{-5/3} \Gamma_0^2 \frac{\delta t_{\text{b}}}{\delta t_{\text{ic}}} \frac{4\pi}{\Omega} L_{\text{b}} \quad (5)$$

where subscripts ic and b refer to the boosted and break out quantities, respectively. When the boosted duration δt_{ic} is dominated by curvature effects, we have $L_{\text{ic}} \approx 0.3\theta\Gamma_0^4 L_{\text{b}}$. The above observational signatures would be present even if Γ_0 is low, as expected for stars in which the jet either fails to maintain sufficient collimation or loses a significant amount of energy before breaking out of the star.

3 OBSERVABLE PRECURSOR EFFECTS

The prompt thermal signal emerging from shock break-out would precede by $\approx \Delta/c \approx 6 \theta_{-1} r_{*,13}$ seconds the prompt emission produced through the Compton drag process. In most cases, and especially if we consider the BATSE [20-600] keV spectral window, the break out emission is too soft to be detected (see equation 1). For compact star progenitors ($r_* < 10^{12}$ cm), however, the break out emission could be detectable with instruments like Ginga and the *BeppoSAX* wide field cameras (see Section 3.1). The boosted component, on

the other hand, could be hard and may be difficult to disentangle from the internal shock emission. In fact, this up-scatter emission should appear as a transient signal $(r_\gamma - r_*)/(2c\Gamma_0^2)$ seconds prior to the main burst, where $r_\gamma = \max(r_\tau, r_{\text{int}})$ is the radius at which the γ -rays are produced and r_{int} is the radius of internal shocks. As shown by equation 2, the radius of transparency of the fireball is likely to happen at some distance from the stellar surface and thus the time delay between the up scatter emission and the burst is given by $r_\tau/(2c\Gamma_0^2) \approx 0.3 \theta_{-1}^{-1} E_{j,51}^{1/2} \Gamma_{0,2}^{-5/2}$ s. If some bursts are characterised by low-intermediate Lorentz factors, precursors with typical photon energies $h\nu \sim 100 \Gamma_{0,1}^2$ keV should have been observed by BATSE $\sim 100 \Gamma_{0,1}^{-5/2}$ s before the main event. Such precursors may have indeed been observed (Koshut et al. 1995).

Fig. 2 shows the break out emission of a fireball propagating through the stellar envelope expected at the end of the evolution of a $25 M_\odot$ main-sequence star (model A01 of MWH01). The effect of a strong, spherically symmetric shock that breaks through the stellar surface is calculated using the non-relativistic hydrodynamics KEPLER code. The equivalent isotropic energy of the fireball pushing the stellar envelope is⁴ $E_{4\pi} \approx 10^{54}$ erg. Due to the low efficiency of semi-convective mixing, the main sequence star ends its life with a relatively large hydrogen envelope ($r_* \approx 9 \times 10^{13}$ cm). In this case, the short duration of the jet, which is limited by a gas fall-back time onto the central black hole, prevents the fireball from acquiring a large bulk Lorentz factor ($\Gamma_0 \approx 5$). An asymmetric supernovae and a weak GRB may result from such explosions. Fig. 3 shows the three component bolometric lightcurve for a mildly beamed burst with intermediate Lorentz factor. The break-out, boosted and internal shock components are shown (see the caption for more details).

3.1 GRB 900126

On 1990 January 26, the Ginga experiment discovered X-ray emission in the 2–10 keV energy range ~ 10 s before the onset of a γ -ray event (Murakami et al. 1991). The γ -ray signal shows two distinct peaks, separated by ~ 6 s, both of which have rise times of ≈ 1.5 s. The peak energy values in the γ -ray emission vary from ≈ 120 keV in the first peak to ≈ 80 keV in the second. The spectrum of the precursor X-ray emission can be described by that of a black body with a temperature $kT = 1.58 \pm 0.26$ keV and a flux $F \sim 2.5 \times 10^{-9}$ erg cm $^{-2}$ s $^{-1}$

⁴ While these calculations are one dimensional, they should roughly simulate the conditions experienced by stellar regions within solid angles that are being pushed by these equivalent isotropic energies, as described by MWH01.

(Murakami et al. 1991). The peak luminosity of the first spike is $\sim 9.5 \times 10^{-6}$ erg cm $^{-2}$ s $^{-1}$, i.e. ~ 2600 times brighter than the thermal precursor.

Knowing the flux and observed temperature of the thermal precursor, it is possible to estimate the radius r_s of the emitting surface as a function of redshift. In the redshift range $0.5 < z < 10$, we obtain $10^{11} < r_s < 3 \times 10^{11}$ cm. In the framework of the shock break out, the radius of the emitting surface is given by $r_s \approx r_*\theta$ and the thermal precursor should precede the boosted emission by $0.2r_*\theta(1+z)/c \approx 2(1+z)$ s. The first peak of the γ -ray emission is indeed observed several seconds after the thermal precursor. If this second peak is interpreted as the Compton boosted emission described above, we can derive the Lorentz factor from the peak frequency of the second pulse and the temperature of the precursor, yielding $\Gamma_0 \approx 8$. The expected ratio of luminosity between the thermal precursor and the boosted pulse would then be $\approx 2500\theta$, to be compared with the measured value of ≈ 2600 . This would consequently imply that the fireball of GRB900126 was only moderately beamed and the radius of the progenitor star was $r_* \approx 10^{11}$ cm. The expected shock break out temperature is (see equation 1) $\approx 1(E_{j,51}/\Delta t_{j,2})^{1/4}$ keV, so that a comparison with the observed $T \approx 1.6(1+z)$ keV implies a total energy of few $\approx 10^{52}$ erg. The fluence of the burst was $\mathcal{F} = 4 \times 10^{-5}$ erg cm $^{-2}$ which, for a $z = 1$ burst with a mild ($\theta \approx 1$) beaming, corresponds to $E_j = 5 \times 10^{52}$ (Fig. 3). On the contrary, if the softening between the first and second γ -ray peaks is caused by the same mechanism that is responsible for both of these emissions (i.e. internal shocks), the lack of detection of the Compton drag transient in the 1.5–400 keV band would imply that $\Gamma_0 \geq 20$.

4 FIREBALL KINEMATICS AND e^\pm PAIR LOADING

Here we quantitatively estimate the predicted spectrum of the prompt transient that arises from the interaction of a fireball with the break-out emission using the framework established by G01 and give a simplified discussion of the generic effects of pair formation. We assume that the photon field inside the stellar cocoon is not very dense and thus the Compton drag process is not efficient until the fireball reaches the shocked plasma region⁵.

Beyond the stellar surface and in the region where the fireball remains optically thick

⁵ The Compton drag effect when the fireball propagates in a funnel embedded in a very dense photon bath has been invoked by L00 and G01. In this scenario, the fireball experiences efficient Compton drag as it reaches the end of the funnel. At this end, the soft photon energy is determined by the stellar surface temperature.

($r < r_\tau$), the total energy emitted by the fireball through the Compton drag process over a distance dr is

$$dE(r) = \frac{\pi}{2} \theta^2 r^2 a T_s^4 \left(\frac{r}{r_*} \right)^{-\alpha} \Gamma^2(r) dr, \quad (6)$$

where the dynamics of the fireball obey

$$M_j c^2 \frac{d\Gamma(r)}{dr} = \frac{\pi}{2} \theta^2 r^2 a T_s^4 \left(\frac{r}{r_*} \right)^{-\alpha} \Gamma^2(r) \quad (7)$$

as long as most of the fireball energy is lost in the Thomson regime (G01). For simplicity, as the scattering rate is $\propto (1 - \beta \cos \theta) \propto (r/r_*)^{-2}$ and the radiation energy $U(r) \propto (r/r_*)^{-2}$, we assume⁶ $\alpha \approx 4$.

The resulting spectrum and the dynamics of the fireball can be strongly affected by the production of e^\pm pairs through $\gamma\gamma$ interactions. e^\pm pairs can be produced by Compton drag photons interacting with the isotropic break-out emission or with each other. This latter interaction can be between photons among the beam or with a seed fraction of back-scattered photons. $\gamma\gamma$ collisions among the beam occur between photons of equal age (cascade shower; Burns & Lovelace 1982; Svensson 1986) and can only affect the high energy tail of the spectrum if $\Gamma_0 \Theta_s > \frac{1}{3}$ (Svensson 1987, G01).

The very high energy emission produced by the Compton drag can also interact with the soft break out photons and produce e^\pm pairs. However, the number of target photons able to interact with the high energy γ -rays to produce pairs strongly decreases beyond r_* . To illustrate the importance of this interaction, we calculate the observed Compton-drag spectrum, taking into account this photon-photon absorption. The observed spectrum ($r_* < r < r_\tau$) is then given by

$$E(\epsilon) = \frac{\pi^2}{4} m_e c^2 \left(\frac{m_e c}{h} \right)^3 \int_{r_*}^{r_\tau} \frac{r^2 (r/r_*)^{-\alpha} e^{-\tau_{\gamma\gamma} \epsilon^3}}{\Gamma^6(r) (e^{\epsilon/\Theta_c} - 1)} dr, \quad (8)$$

where $\Theta_c = 2\Gamma^2 \Theta_s$, ϵ is the photon energy in units of $m_e c^2$ and $\tau_{\gamma\gamma}$ is the photon-photon optical depth of Compton drag photons interacting with the soft break-out emission (see equations 11, 12 and 13 of G01). In Fig. 4 we show three examples of both the predicted spectrum and the Γ profiles corresponding to different values of the stellar envelope and the total fireball energy. The resulting spectrum is calculated with and without the absorption term $e^{-\tau_{\gamma\gamma}}$ (shaded region). If the Compton drag process is efficient ($\xi \propto r_*$, see equation 3), the fireball decelerates and the observed spectrum is the convolution of all the locally

⁶ It is also plausible that $U(r) \times (\text{scattering rate})$ can have a more complex profile for which $2 < \alpha < 4$, as described in G01

emitted spectra. Beyond r_* the photon density is strongly reduced, thus further decreasing both the efficiency of the Compton drag process and the amount of energy absorbed in $\gamma\gamma$ collisions.

As can be seen in Fig. 4, the radiation absorbed by $\gamma\gamma$ interaction between beam photons and break-out radiation is small. However, the resulting spectra are hard, with a significant fraction of the energy above the $\gamma\gamma \rightarrow e^\pm$ formation energy threshold; and a high compactness parameter can result in additional pairs being formed outside the stellar radius (MT00; TM00).

When the integrated flux of photons of energy $\epsilon > 1$ is large, each side-scattered photon deposits its entire momentum, along with the momentum of the interacting beam photon, into an e^\pm pair. The pairs (together with the ions) start being accelerated to $\Gamma_\mu \geq 1$ (provided that the pairs remain coupled to the baryons; TM00). Particles are accelerated away from the stellar surface as long as $\Gamma_\mu < \Gamma_{\text{eq}}$, where

$$\Gamma_{\text{eq}}(r) \approx 3^{1/4} \frac{r}{r_*} \quad (9)$$

is the equilibrium Lorentz factor close to the extended source (MT00). Bulk motion starting with $\Gamma_\mu(r) > \Gamma_{\text{eq}}$ is quickly decelerated to $\Gamma_\mu \approx \Gamma_{\text{eq}}$. This saturation of the Lorentz factor is due to the drag caused by the aberration into the forward hemisphere of blue-shifted photons as seen in the particle rest-frame. Large values of Γ_μ can only be obtained for particles injected at distances beyond the critical radius

$$r_c \approx 0.8(lm_e/\mu)^{1/4}r_*, \quad (10)$$

at which drag caused by the radiation field is negligible ($lm_e/\mu = L\sigma_T/(4\pi\mu c^3 r_*)$ is the rescaled compactness parameter and μ is the mean mass per scattering charge, see MT00). At a distance $r > r_c$ in front of the radiation source, $e^\pm + \text{ions}$ can be accelerated to a maximum value of Γ_μ satisfying

$$\Gamma_\mu \approx \begin{cases} \left(\frac{3lm_e r_*}{4r\mu}\right)^{1/3} & \frac{2}{3}\Gamma_\mu^2 c\delta t_{\text{ic}} > r \\ \frac{l\delta t_{\text{ic}} c r_*}{r^2} & \text{otherwise.} \end{cases} \quad (11)$$

The maximum Lorentz factor Γ_μ is shown in Fig. 5. The e^\pm pair loading process depends only on the “seed” γ -ray photon, while its manifestations are consequences of the external density and on the initial bulk Lorentz factor (Mészáros et al. 2001). The external baryon density n_{ext} determines the optical depth that can be built up through back-scattering and pair multiplication. For a fixed Lorentz factor Γ_0 , the external density determines when the

outer shock and the reverse shock become important and whether this happens within the radius already polluted with pairs (MT00; TM00; Mészáros et al. 2001).

For small values of ξ , the e^\pm pair-rich external medium would carry less energy and inertia than the erupting fireball itself, and therefore start to decelerate at a smaller radius than the collimated fireball, so that the latter would overtake it (Mészáros et al. 2001). On the other hand, if the Compton drag process dominates, the pair energy can exceed that of the collimated fireball (after kinetic energy has been extracted from it), substantially altering the usual properties of the deceleration shocks and the afterglow emission. In this case, the afterglow would be dominated by the emission of the accelerated medium and not by the decelerated fireball. The lepton/proton fraction in the ejecta can then be much larger than normal, causing the radiation to be much softer than in the usual model, because the same energy density has to be shared among a larger number of particles. Pair production can also increase the optical depth outside of the shocks, and both the Compton drag and the internal shock emission may be modified by Comptonization. We plan to investigate these possibilities and their consequences for the predicted prompt and afterglow emissions in future work.

5 SUMMARY

Many massive stars produce supernovae when forming neutron stars in spherically symmetric explosions, but some may fail neutrino energy deposition, forming a black hole in the centre of the star and possibly a GRB (MW99). One expects various outcomes ranging from GRBs with large energies and durations, to asymmetric, energetic supernovae with weak GRBs. The prompt transients produced by the Compton drag of the shock break-out emission would provide a natural test to distinguish between these different stellar explosions. The detection of these prompt multi-wavelength signatures would be a test of the collapsar model; and the precise measurement of the time delay between emissions would constrain the dimensions of the stellar progenitor, the Lorentz factor of the fireball and the radius of the burst emitting region (r_{int} or r_τ).

This very hard prompt emission would propagate ahead of the collimated fireball loading the external medium with e^\pm pairs. In most early discussions (TM00; Madau et al. 2000; Mészáros et al 2001; Belobodorov 2002), the concern has been raised that e^\pm pair loading in low-density environments is rather inefficient, converting only a few percent of the bulk

motion energy into e^\pm pairs. We have shown here that the Compton drag mechanism can be an effective catalyst for converting bulk motion energy into γ -rays close to the stellar surface. Numerous e^\pm pairs can then be produced as some of the photons in the beam are backscattered and interact with other incoming photons. The process discussed here suggests that the e^\pm pairs can play a substantial role in both the dynamics of the fireball and the nature of the afterglow emission, as they are produced well before the fireball becomes optically thin. This suggests that if GRBs are the outcome of the collapse of massive stars involving a relativistic fireball jet, the time structure, dynamics and efficiency of the prompt and afterglow emissions may have a more complex dynamic than the standard models suggest.

ACKNOWLEDGEMENTS

We thank A. Celotti, P. Madau, P. Mészáros, G. Morris, S. Woosley, A. Heger and W. Zhang for many helpful conversations. We are particularly grateful to M. J. Rees for numerous insightful comments and suggestions. ERR thanks the UCSC Department of Astronomy and Astrophysics for its hospitality and acknowledges support from CONACYT, SEP and the ORS foundation. A.M. acknowledges support from DOE ASCI (B347885).

REFERENCES

Aloy M. A., Ibanez J. M., Marti J. M., Muller E., MacFadyen A. I., 2000, *ApJ*, 531, L119
 Amati L. et al., 2000, *Science*, 290, 953
 Beloborodov A. M., 2002, *ApJ*, 565, 808
 Bloom J. S. et al., 1999, *Nature*, 401, 453
 Bloom J. S., Kulkarni S. R., Djorgovski S. G., 2001, *ApJ* submitted (astro-ph/0010176)
 Burns M. L., Lovelace R. V. E., 1982, *ApJ*, 262, 87
 Chevalier R. A., 1982, *ApJ*, 259, 302
 Colgate S. A., 1974, *ApJ*, 163, 221
 Dermer C., Böttcher M., 2000, *ApJ* 534, L155
 Eichler D., Livio M., Piran T., Schramm D. N., 1989, *Nature*, 340, 126
 Fruchter A. S., 1999, *ApJ*, 516, 683
 Fruchter A. S. et al., 1999, *ApJ*, 520, 54
 Ghisellini G., Lazzati D., Celotti A., Rees M. J., 2001, *MNRAS*, 316, L45 (G01)
 Katz J., 1994, *ApJ*, 422, 248
 Klužniak W., Lee W. H., 1998, *ApJ*, 494, L53
 Koshut T. M., Kouveliotou C., Paciesas W. S., van Paradijs J., Pendleton G. N., Briggs M. S., Fishman G. J., Meegan C. A., 1995, *ApJ*, 452, 145
 Kulkarni S. R. et al., 1998, *Nature*, 395, 663

Lattimer J. M., Schramm D. N., 1976, *ApJ*, 210, 549

Lazzati D., Ghisellini G., Celotti A., Rees M. J., 2000, *ApJ*, 529, L17 (L00)

Lazzati D. et al., 2001, *A&A*, 378, 996

Lee W. H., Klužniak W., 1999, *ApJ*, 526, 178

MacFadyen A. I., Woosley S. E., 1999, *ApJ*, 524, 262 (MW99)

MacFadyen A. I., Woosley S. E., Heger A., 2001, *ApJ*, 550, 410 (MWH01)

Madau P., Thompson C., 2000, *ApJ*, 534, 239 (MT00)

Madau P., Blandford R., Rees M. J., 2000, *ApJ*, 541, 712.

Mészáros P., 2001, *Science*, 291, 79

Mészáros P., Rees M. J., 1997, *ApJ*, 476, 232

Mészáros P., Ramirez-Ruiz E., Rees M. J., 2001, *ApJ*, 554, 660

Mészáros P., Waxman E., 2001, *Phys. Rev. Lett.*, 87, 1102

Murakami T. et al., 1991, *Nature*, 350, 592

Paczyński B., Xu G., 1994, *ApJ*, 427, 708

Paczyński B., 1998, *ApJ*, 494, L45

Piro L. et al., 2000, *Science*, 290, 955

Ramirez-Ruiz E., Trentham N., Blain A., 2002, *MNRAS*, 329, 465

Rees M. J., Mészáros , P., 1992, *MNRAS*, 258, 41

Rees M. J., Mészáros , P., 1994, *ApJ*, 430, L93

Rees M. J., 1999, *A&AS*, 138, 491.

Reichart D. E., 1999, *ApJ*, 521, L111

Ruffert M., Janka H.-T., Takahashi K., Schaefer G., 1997, *A&A*, 319, 122

Sari R., Piran T., 1995, *ApJ*, 455, L143

Svensson R., 1986, *IAU Coll. No. 89*, eds Mihalas D. & Winkler, p. 325

Svensson R., 1987, *MNRAS*, 227, 403

Thompson C., Madau .P., 2000, *ApJ*, 538, 105 (TM00)

Woosley S. E, 1993, *ApJ*, 405, 273

Wheeler J. G., Yi I., Hofflich P., Wang L., 2000, *ApJ*, 537, 810

This paper has been typeset from a *TeX*/ *L^AT_EX* file prepared by the author.

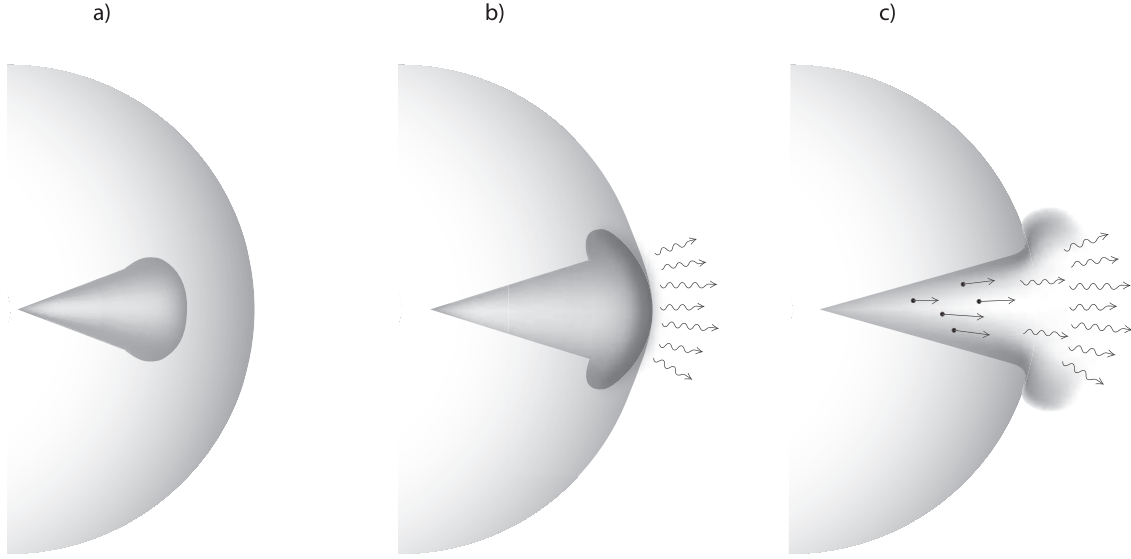


Figure 1. Diagram illustrating the propagation of the jet through the stellar mantle. Initially, the jet is unable to move the envelope material to a speed comparable to its own and thus is abruptly decelerated. As the jet propagates a bow shock runs ahead of it (a). The bow shock of the jet will both heat material and cause it to expand sideways. A strong thermal precursor is produced as the shock breaks through the stellar surface and exposes the hot shocked material (b). The fireball escapes the stellar envelope and interacts with very dense soft photon emission (c), converting the fireball bulk energy into radiation with a remarkably high efficiency.

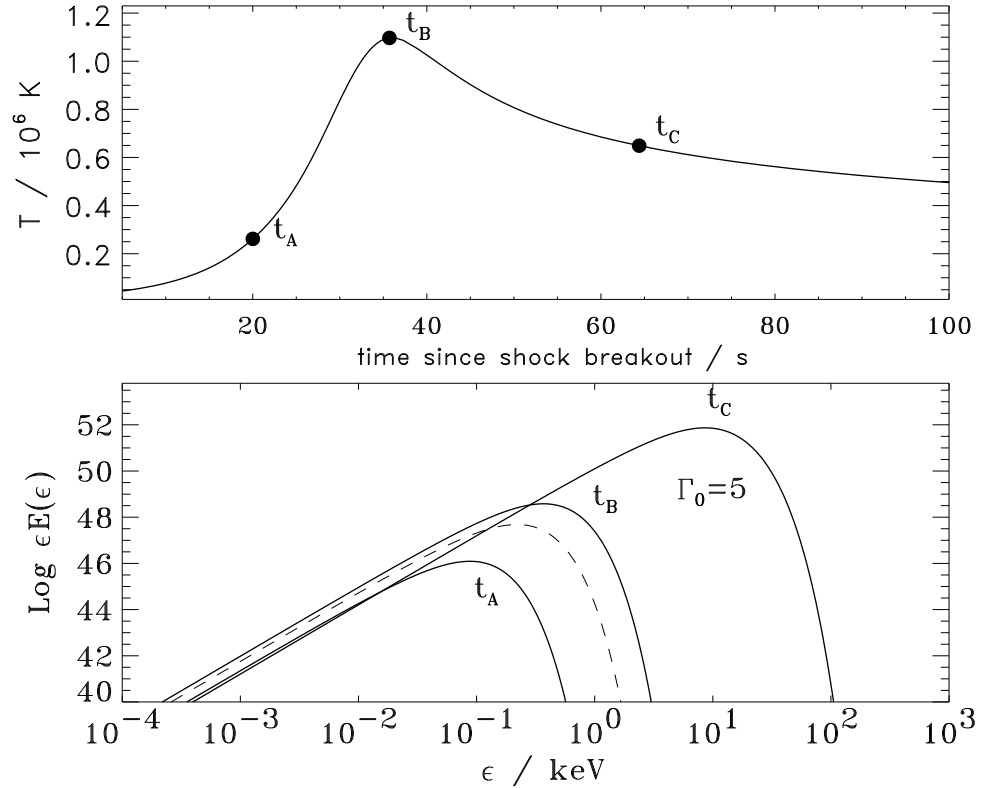


Figure 2. Shock break-out and Compton-dragged prompt emission in core collapse explosions. The stellar progenitor A01 of MWH01 is used as the initial model, a pre-supernova star of initial mass $M_i = 25 M_\odot$ that ended its life with a low-density hydrogen envelope of $6.57 M_\odot$ and a stellar radius of $\approx 9 \times 10^{13}$ cm. Upper panel: the effective temperature as a function of time since shock break out. Lower panel: examples of the the black-body spectra during the initial phase (t_A and t_B) before the impact of the jet ($E_{4\pi} \approx 10^{54}$ and $\theta = 0.6$). The fireball interacts with the dense thermal emission at a time $t_c = \Delta/c$, boosting photons by $\approx 2\Gamma_0 \approx 2(5)^2$ in frequency. The dashed line corresponds to the emission at t_c neglecting the Compton drag process.

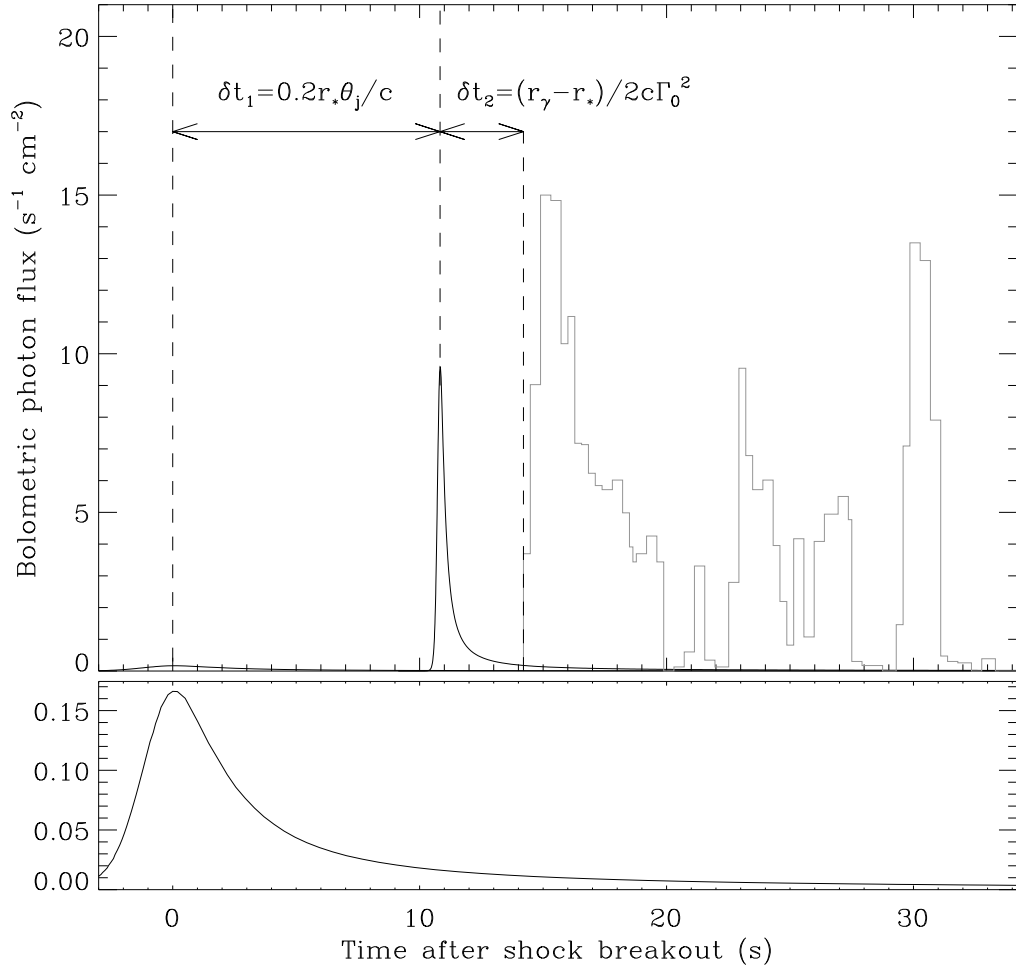


Figure 3. Lightcurve of the break-out, Compton-drag and internal shock components of a GRB. The lightcurve is computed to match the observation of GRB900126: $r_* = 8 \times 10^{11} \text{ cm}$, $\theta = 0.9$, $E_j = 3 \times 10^{51} \text{ erg}$, $\Delta t_j = 20 \text{ s}$, $\Gamma_0 = 8$ and for a redshift $z = 1$. The main panel shows all the three components of the lightcurve while the lower panel shows a close up of the break out component.

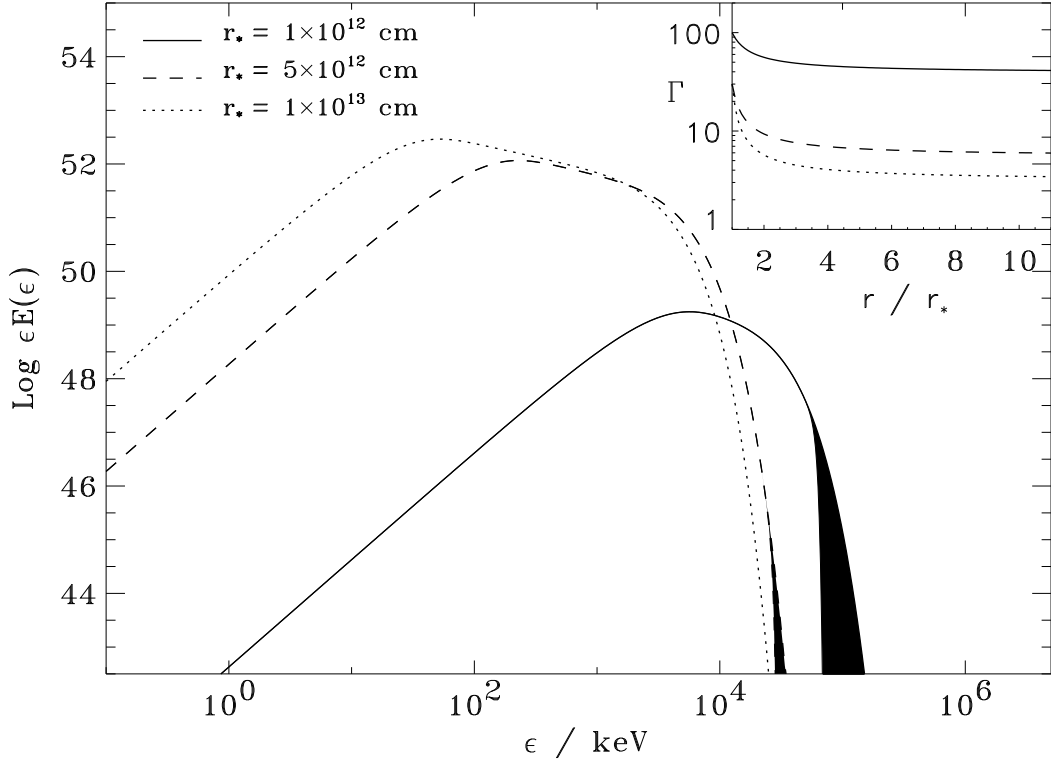


Figure 4. Examples of spectra produced by the interaction of a collimated fireball with the break-out emission. The inset panel shows the corresponding bulk Lorentz factor. The model parameters are: $E_j = 10^{51}$ erg (solid line), 5×10^{52} erg (dashed and dotted lines); $\theta = 0.2$ (solid line) and 0.1 (dashed and dotted lines). In all cases we assume $\Delta t_j \approx 10^2$ s and $\alpha = 4$. The shaded regions correspond to the emission absorbed by $\gamma - \gamma$ interaction between beam photons and break-out radiation.

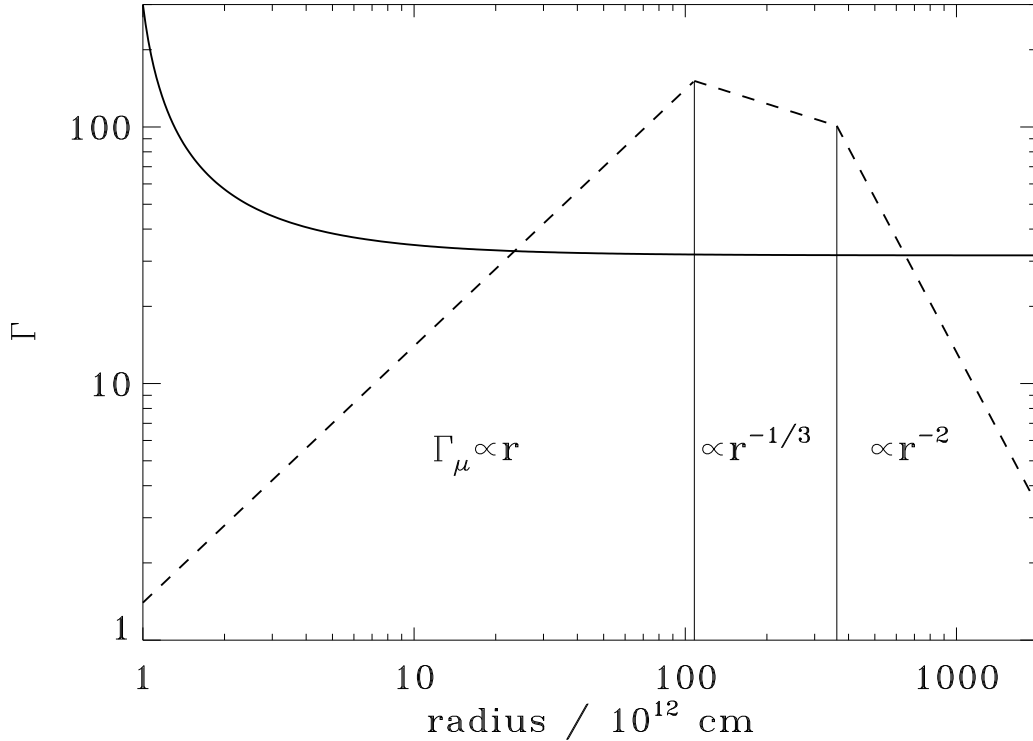


Figure 5. Plot of the maximum ($e^\pm + \text{ions}$) bulk Lorentz factor Γ_μ as a function of radius (dashed line). The model parameters are: $E_j = 10^{51}$ erg, $\theta = 0.1$, $r_* = 10^{12}$ cm, $\Delta t_j \approx 10^2$ s, $\delta t_{ic} = \lambda/c$ and $\mu \approx m_p$. The solid line gives the profile of the bulk Lorentz factor of the fireball decelerated by the Compton drag mechanism. When pairs are produced in sufficient numbers, the mean mass per scattering charge drops to $\mu \approx m_e$ and acceleration can be more efficient.